Assessment of the putative binding conformation of a pyrazolopyridine class of inhibitors of MAPKAPK2 using computational studies

ARTICLE *in* EUROPEAN JOURNAL OF MEDICINAL CHEMISTRY · SEPTEMBER 2009

Impact Factor: 3.45 · DOI: 10.1016/j.ejmech.2009.09.030 · Source: PubMed

3 AUTHORS, INCLUDING:

Rajni Miglani
University of Strathclyde
3 PUBLICATIONS **57** CITATIONS
SEE PROFILE

Voleti Sreedhara Rao
TheraXel Discoveries
20 PUBLICATIONS **217** CITATIONS
SEE PROFILE

European Journal of Medicinal Chemistry 45 (2010) 98–105

Contents lists available at ScienceDirect

European Journal of Medicinal Chemistry

journal homepage: http://www.elsevier.com/locate/ejmech

Original article

Assessment of the putative binding conformation of a pyrazolopyridine class of inhibitors of MAPKAPK2 using computational studies

Rajni Miglani [a], Ian A. Cliffe [b], Sreedhara R. Voleti [c,*]

[a] Division of Molecular Modeling, New Drug Discovery Research, Ranbaxy Laboratories Limited, Sector-18, Gurgaon – 122001, India
[b] Department of Medicinal Chemistry, New Drug Discovery Research, Ranbaxy Laboratories Limited, Sector-18, Gurgaon – 122001, India
[c] Institute of Life Sciences, University of Hyderabad Campus, Gachibowli, Hyderabad – 500040, India

ARTICLE INFO

Article history:
Received 14 September 2008
Received in revised form
25 July 2009
Accepted 17 September 2009
Available online 30 September 2009

Keywords:
MAPKAPK2 (MK2)
Kinase
Pyrazolopyridines
Pyrazolopyrimidine

ABSTRACT

The Ser/Thr protein kinase MAPKAP kinase2 (MAPKAPK2 or MK2) plays an important role in inflammation. A comparison of several crystal structures of MK2 shows that differences in active and inactive conformations result in large part from structural variations within the conformations of the glycine rich loop (p-loop) regions. We propose the most preferred binding conformation of two classes of MK2 inhibitors and suggest plausible critical interactions with active site residues. The predicted binding conformations of the two classes of MK2 inhibitors depend upon their orientation in the active site and activities were well correlated with the sum of D and G scores. A qualitative relationship between the sum of D and G scores and the measured activities can be demonstrated.

1. Introduction

Kinases are reported to be involved in a plethora of diseases and it is estimated that approximately one-third (20–30%) of all drug discovery programs target protein kinases [1]. Mitogen-activated protein kinases (MAPKs) belong to the Ser/Thr kinase family [2]. The MAPK family can be separated into three major subgroups, viz. extracellular signal-regulated kinases (ERKs), c-Jun N-terminal kinases (JNKs)/stress-activated protein kinases (SAPKs), and p38/reactivating kinases (RK) [3]. JNK and p38 kinases are responsive to inflammatory cytokines, bacterial lipopolysaccharide, and environmental stresses such as osmotic shock, ionizing radiation, and ischemic injury, whereas activators of ERK1/2, including mitogens, growth factors, and hormones, act through receptor tyrosine kinases [4]. MAPKs, in turn, catalyze the phosphorylation and activation of several downstream substrates including MAPKAP kinases, phospholipases, transcription factors, and cytoskeletal proteins [5]. MK2 is a member of the p38 MAP kinase pathway with p38 as its main cellular activator [6,7]. The p38/(MK2) cascade regulates the synthesis of tumor necrosis factor-α (TNF-α) and other pro-inflammatory cytokines such as interleukin-6 (IL6), and interferon-γ (IFn-γ), and is thus attractive as a potential drug target for inflammatory diseases [8,9].

A knockout study of MK2 in mice revealed reduced levels of TNF-α, IFn-γ, IL-1β, and IL-6 and an increased survival upon challenge with LPS, suggesting that MK2 is a key regulator of the inflammatory process [10]. Observations have also suggested that a selective MK2 inhibitor may demonstrate efficacy equal to that of a p38 inhibitor without affecting additional cellular pathways governed by p38 that may lead to undesirable side-effects [11]. Various MK2 inhibitors have been reported in the literature and some of them were found to be very active. Table 1 shows a selection of reported classes of inhibitors along with corresponding literature references and activities.

Despite the substantial achievements in protein kinase drug discovery, the design of potent inhibitors with a high degree of selectivity during lead optimization remains a major challenge. Systematic analysis of the crystal structures of protein kinases can offer some insights into the design of selective inhibitors, while the non-availability of such information makes the challenge more difficult. Thus, a co-crystal conformation of an inhibitor with a protein kinase would help in the design of novel inhibitors.

In this report, we analyze different features in the crystal structures of MK2, i.e. the conformational flexibility of the active site, the reorganization of the glycine rich loop/phosphate-binding loop/p-loop upon ligand binding (i.e. residues G71–G76 which contain the highly conserved ATP binding motif GKGING),

* Corresponding author. Tel.: +91 40 66571500; fax: +91 40 66571581.
E-mail addresses: rajni.miglani@gmail.com (R. Miglani), Sreedharav@ilsresearch.org (S.R. Voleti).

0223-5234/$ – see front matter © 2009 Elsevier Masson SAS. All rights reserved.
doi:10.1016/j.ejmech.2009.09.030

Table 1
Classes of MK2 inhibitors.

Series	MK2 inhibition (IC_{50})
Indazole carboxamide [12]	<150 μM
1,2-Substituted cyclic derivatives [13]	–
Oxazolyltriazolo pyridines [14]	<10 μM
Pyrazolo[1,5-*a*]pyridine [15]	<0.2 μM, 'active' to 'very active'
Pyrazolo[1,5-*a*]pyrimidines [16]	≤2 μM, 'active' to 'very active'
Aminocyanopyridines/ benzopyranopyridines [17–20]	>0.1 μM
Acyclic pyrazoles [21]	>0.02 μM
Pyrrolo[3,2-*c*]pyridinones [11,22]	>0.005 μM
Carboline analogs [23]	~10 nM

difference in α-C helix and the change in the shape of the active site resulting from inactive and active conformations of MK2.

We also propose the putative binding conformations of a series of pyrazolo[1,5-*a*]pyridine inhibitors [15] of MK2 having the general structure shown in Fig. 1, **(1)** and make an attempt to correlate activities with total scores and binding conformations. We also analyze other MK2 inhibitors belonging to a similar structural class, i.e. pyrazolo[1,5-*a*]pyrimidines [16].

2. Computational methodology

Docking experiments were carried out using Surflex in the SYBYL7.3 molecular modeling package installed on a Silicon Graphics Fuel workstation running on the IRIX6.5 operating system. Surflex is a docking module which employs an idealized active site ligand called a *protomol* as a target to generate putative poses of molecules or molecular fragments. The putative poses are scored using the Hammerhead scoring function which also serves as an objective function for local optimization of poses [24–26]. Flexible docking precedes either by incremental construction from high-scoring fragments as in Hammerhead or by a crossover procedure that combines pieces of poses from intact molecules. This fragment assembly method is loosely related to genetic algorithm approaches, but it is deterministic [27,28].

3. Results and discussion

3.1. Selection of data set

Pyrazolo[1,5-*a*]pyridines from four different categories were chosen according to their reported activity ranges, i.e. <0.2 μM (++++), 0.2–1 μM (+++), 1–10 μM (++), and 10–100 μM (+). Various molecules containing diverse groups in place of R1, R2, and R3 were considered. The majority of the changes occurred at the R3 position and major changes in activity can be attributed to substituents at this position {structures with their activities are shown in Supplementary data}. Substitutions at the R1 position were mainly aromatic in nature [such as phenyl, substituted phenyl, 4-methoxyphenyl, 4-ethoxyphenyl, (2-methoxyethoxy)phenyl, 2-methoxyphenyl, chlorophenyl, biphenyl, benzthiazole, substituted benzthiazole, 2-methylbenzthiazole, 2-ethylbenzthiazole, etc.]. At the R2 position, the substituents were mainly alkyl groups [such as methyl, ethyl, propyl, butyl, cyclopropyl, isopropyl and phenyl, propene, isobutyl, etc.]. Basic amine containing substituents were located at the R3 position [such as piperidine, 4-aminocyclohexyl, cyclohexyl isobutyl amine, ethylamine, propylamine, pentylamine, hexylamine, benzylcyclohexylamine, cyclohexyl methylamine, cyclohexylphenethyl amine, cyclohexyl (3-phenylpropyl)amine, 3-cyclohexylamine, pyrrolidine, and tetrahydroisoquinoline, etc.]

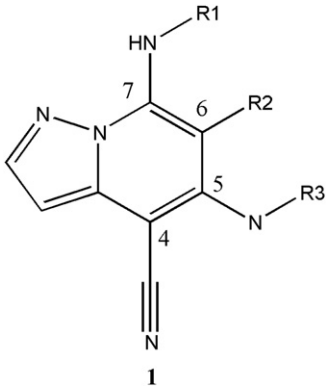

1

Fig. 1. General structure of compounds **1** from WO2006/109867A1, wherein R1, R2, R3 represent different substituents.

3.2. Crystal structure analysis

X-ray crystal structures of the MK2 kinase domain are available in the Protein Data Bank [29] and one is reported in a patent with a non-hydrolysable ATP analog (ANP, **2**) [30]. We have compared the X-ray crystal structures of the kinase domains of MK2 in an apo form; bound to Staurosporin (**3**), ADP (**4**), and a carboline analog (**5**); and bound to two other inhibitors (**6** and **7**), as shown in Fig. 2. Another potent inhibitor of MK2 (**8**) is also shown in Fig. 2 for its close structural similarity with the inhibitors **6** and **7**. The MK2 kinase core domain contains an overall fold that is very similar to the structures of other protein kinases.

The inactive kinase conformation of the apo form of MK2 (1KWP) shows an open ATP pocket. The substrate-binding site is blocked by the C-terminal autoinhibitory region which takes the form of a helix [31]. The co-crystal structures with Staurosporin (**3**, 1NXK) and ADP (**4**, 1NY3) reveal the active conformation of MK2, in which the ATP binding site adopts a relatively closed conformation with a narrow and deep cleft [32]. The crystal structures with pyrrolo[3,2-*c*]pyridinone derivatives and a carboline analog {(**5**, 2PZY, 34 nM), (**6**, 2JBO and 2JBP, 8.5 nM) and (**7**, 2P3G, 126 nM)} also reveal the active conformation of MK2 [22,23,33]. An ionic lock interaction between the conserved lysine and glutamate residues from helix αC represents a hallmark of the active conformation of protein kinases [34], and a similar interaction has been observed between the conserved K93 and E104 residues of the active conformation of MK2 (as seen in the crystal structures 2JBO, 2JBP, 1NXK and 2PZY).

The root mean square distance is less than 1.5 Å of the active conformations of MK2 (C-α trace), as shown in Fig. 3a. Comparison of all the aligned crystal structures reveals an overall larger movement in the C-terminal domain than in the N-terminal domain. The most significant differences lie in the β-sheets which contain the highly conserved glycine rich-motif GLGING i.e., G71–G76 or the p-loop which is constituted by the β1 and β2 strands in the N-terminal domain (as shown in Fig. 3b). The conserved glycines confer two important structural features upon the p-loop: the interaction of the backbone amides with the phosphate groups of ATP without any steric hindrance, and flexibility in the backbone which allows the p-loop to adopt multiple conformations and thereby act as a flexible clamp for stabilizing the triphosphate group. It is well known that the conformational flexibility of the p-loop plays an important factor in the regulation of the function of many protein kinases [32].

There is a reorganization of the p-loop in all the observed crystal structures. For example, in 1NY3, the crystal structure with ADP, the glycine rich loop is in an open stretched form as compared to the

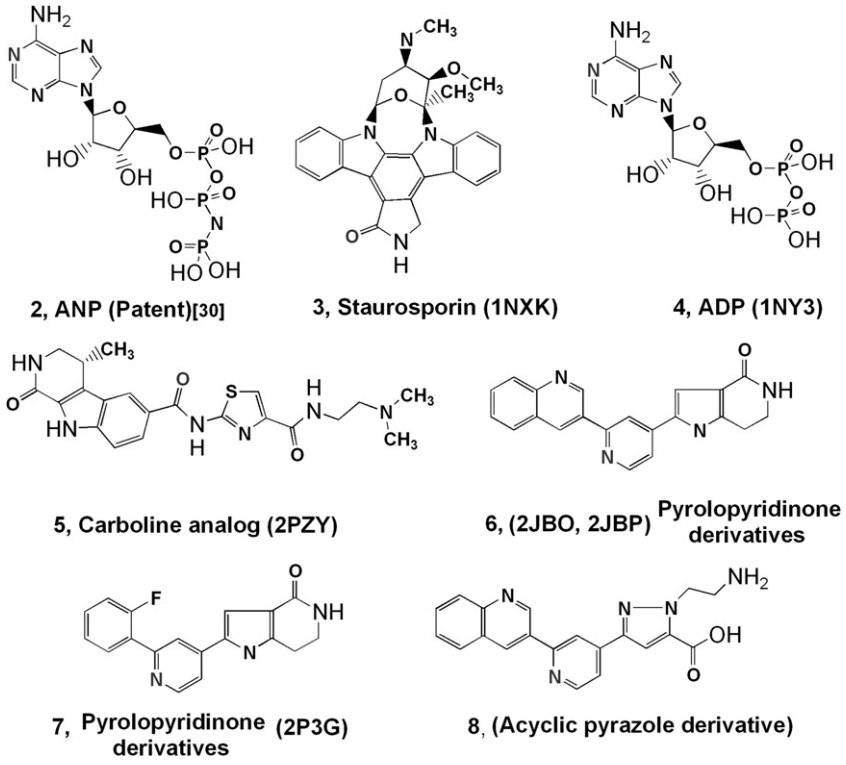

Fig. 2. Various inhibitors of MK2 with PDB codes in parentheses.

crystal structures of **5** (2PZY) and **6** (2JBP) owing to the presence of the phosphate groups of ADP. In the co-crystal structures of inhibitors **5** and **6** (2PZY and 2JBP, respectively), the p-loop is closer to the ligand. However, in another crystal structure with the ligand **6** (2JBO), the closeness of the p-loop to the ligand is blocked by a phosphate anion which is bound adjacent to the inhibitor. In another crystal structure with the inhibitor **7** (2P3G), the p-loop is further removed because the ligand is bound away from the hinge as compared to inhibitors **5** and **6** (2PZY and, 2JBP respectively). Table 2 shows the distances of the same residues in the p-loops of ADP-bound MK2 enzyme and other MK2 crystal structures. The residues of the p-loop of the crystal structures with inhibitors **6** and **7** (2JBO and 2P3G, respectively) are closer in general to the p-loop of the crystal structure with **2** [ADP (1NY3)] than the crystal structures with inhibitors **5** and **6** (2PZY and 2JBP, respectively). A comparison of the inhibitor **3** bound crystal structure (1NXK) with other inhibitor bound MK2 crystal structures, indicates that the glycine rich loop between β strands 1 and 2, and the loop on the other side of β strand 2 that connects to β strand 3 (residues 83–88), has moved extensively. This observation implies that the inhibitor **3** binds much deeper into the active site pocket when compared to other inhibitors. In addition, the distances of p-loop residues in the

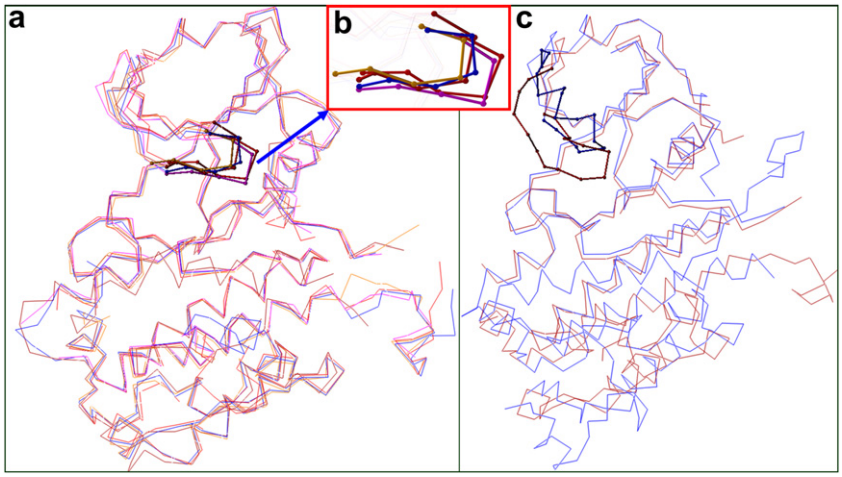

Fig. 3. (a) Overlay of co-crystal structures (2JBO, 2JBP, 1NY3, 2P3G, and 1NXK). The root mean square distance (rmsd) between the five crystal structures is less than 1.5 Å. The main difference between the crystal structures is in the conformation of the glycine rich loop (shown in ball-and-stick) affecting the ATP site. (b) A closer look at the glycine rich motif. (c) Overlay of active (blue 1NY3) vs inactive (brown, 1KWP) MK2 kinase. The rmsd between active and inactive conformation in C-α trace is 4.7 Å.

Table 2
The distances of the same residues in Å in the glycine rich loop (GLGIAG) of different crystal structures as compared with enzyme bound ADP (**2**, 1NY3).

PDB ID	Ligand	Kinase form	G71	L72	G73	I74	A75	G76
1NXK	Staurosporin (**3**)	Active	2.2	3.1	4.1	4.3	3.3	4.3
2PZY	Carobline analog (**5**)	Active	1.8	2.8	2.9	3.8	2.2	3.0
2JBP	Pyrrolopyridinone (**6**)	Active	1.9	2.3	3.3	2.0	3.0	3.8
2JBO	Pyrrolopyridinone (**6**)	Active	2.2	1.8	1.9	1.3	0.8	0.6
2P3G	Pyrrolopyridinone (**7**)	Active	2.3	0.6	1.2	1.3	0.9	1.8
1KWP	Apo	Inactive	12.8	7.9	8.6	16.5	3.1	3.6

Table 3
The torsion angle distribution of the DFG motif residues (Ψ, Φ) in both active and inactive forms of MK2.

S. No.	Conformation	D		F		G	
		Φ	Ψ	Φ	Ψ	Φ	Ψ
1KWP	Inactive	120	13	324	322	241	41
1NY3	Active	141	55	298	320	246	41

inhibitor **3** bound crystal structure are also greater than the corresponding ones of all other active forms of MK2, also corroborating the deep binding of inhibitor **3** to the active site.

The inactive conformation of MK2 (1KWP) shows an rmsd of 4.7 Å in C-α trace when compared with the ADP-bound active MK2, and 5.1 Å when compared with the inhibitor **3** bound MK2, respectively (as shown in Fig. 3c), and suggests a difference in the conformations of MK2. It appears that the β1 strand of the p-loop (N-terminal domain) in the inactive kinase conformation of MK2 adopts a short helical structure (consisting of a helix–loop–β strand conformation instead of the commonly observed β strand–loop–β strand). Both the short helix and the loop connecting the short helix and β2 strand moves inward (vide infra Table 2) leaving a wide open ATP pocket, accessible neither to ATP nor enzyme inhibitors. We are speculating that the conformational change in the p-loop in the N-terminal domain may be part of the MK2 activation process, but there is a possibility that the difference in crystal structures could also be due to the conditions used for crystallization and heavy atom derivatization. It is conceivable that the mercury compounds used for crystallization of the particular crystal structure have led to the disruption of the five-stranded β sheet and a conformational shift of the β1 strand to an α helix (i.e. a sheet helix–loop–β strand conformation instead of the commonly observed β strand–loop–β strand). However, the answer to this question requires further structural studies. On comparing all the MK2 crystal structures, we observed that the α-C helix in the the N-terminal domain is one turn shorter in the auto-inhibited inactive MK2 crystal structures as compared to other MK2 structures which are in the active conformation. Shortening of the α-C helix also confirms the inactive conformation of MK2 kinase.

The inactive MK2 conformation also contains the residues (328–368) which form an autoinhibitory α helix that binds as a pseudo-substrate in the substrate-binding site. This "pseudosubstrate" region is thought to be positioned in a manner that would effectively block the binding of incoming protein and peptide substrates. In the crystal structures of ADP and other MK2 inhibitors, the entire autoinhibitory domain is completely disordered or partially present, thereby allowing peptidic substrates and peptidomimetic inhibitors to bind to MK2.

The shape of the active site of a kinase is influenced by several factors including access to allowed conformational states for the hinge, p-loop, and DFG motif. Such an access also depends on whether or not an inhibitor targets the ATP binding pocket or extends into the hydrophobic pocket [35,36]. In the case of MK2, the shapes of the active sites of both the active and inactive conformations differ due to the changes in the conformations of the glycine rich loop, β1, and β2 sheets, while the gatekeeper residue (M138) and the DFG motif adopt similar conformations. This can be seen from the similar torsion angle distributions of the DFG motif residues (Ψ, Φ) in both the active and inactive forms of MK2, as indicated in Table 3.

An analysis of the binding of ADP and inhibitors **3**, **5**–**8** (for inhibitor **8** we propose the binding conformation through Surflex in developed docking model, shown in Fig. 4a) reveals that the nitrogen atom of the adenine ring of ADP, the carbonyl oxygen atom of the lactam **3**, the carbonyl oxygen atom of the amide 5, and the nitrogen atom of the pyridines **6**–**8** (shown in red in Fig. 2) make hydrogen-bonding interactions with the backbone amide of the hinge residue L141.

The binding conformation of the MK2 inhibitor **5** [23] shows that the dimethylamino-ethylcarbamoyl-thiazolyl-amide is extended towards the solvent exposed area, while the external amide nitrogen atom makes a hydrogen bond with the backbone carbonyl oxygen atom of L70. Additionally, the oxygen and nitrogen atoms of the carboline amide moiety are locked by hydrogen-bonding interactions with K93 and D207, respectively. The thiazole ring is stabilized by the side chain of L70, while the carboline ring is stabilized by the hydrophobic side chains of V78, M138, L193 and T206.

3.3. Validation of co-crystal structures of MK2 through docking

Validation of the docking program Surflex was carried out using ADP bound to the MK2 enzyme (1NY3). Protein was prepared for docking studies using the Biopolymer module in SYBYL, i.e. existing

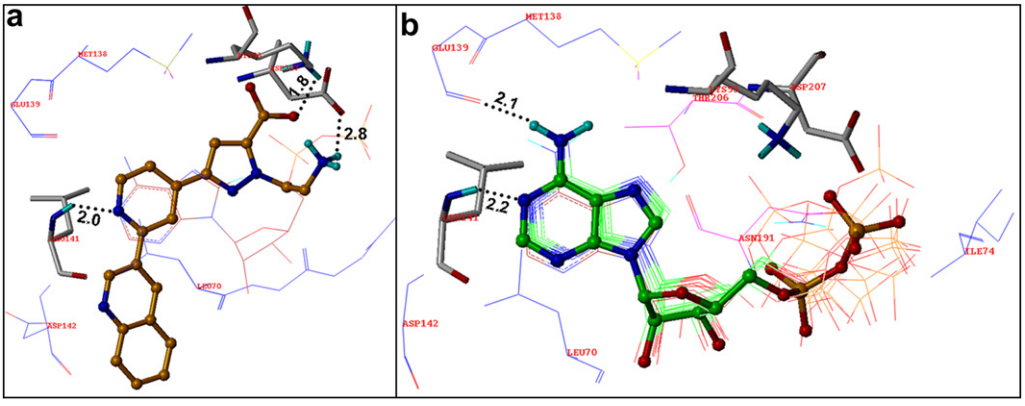

Fig. 4. (a) Putative binding conformation of inhibitor **8** in MK2 enzyme. (b) Docking of ADP (co-crystal conformation C-atom shown in brown color) in MK2 enzyme. Critical residues of MK2 are shown in stick model; generated conformations of ADP are shown in green; hydrogen-bonding interactions are shown in black dotted lines with corresponding distances.

charges and water molecules were deleted from protein; loops were built; hydrogen atoms were added to the protein; and Kollman-all and MMF94 charges were loaded on to the protein and the ligand, respectively. *Protomol* (active site) and sfxc (Surflex descriptor) files were generated based on the position of the ligand ADP using default parameters, i.e. bloat – 0 Å and threshold – 0.50. ADP was drawn in SYBYL7.3 and MMF94 charges were added.

It was found that Surflex was able to reproduce the co-crystal conformation of ADP (as shown in Fig. 4b) along with the other conformations. All the conformations fit into the same volume as that of the co-crystal orientation of ADP with a total top consensus score of 4.9. The phosphate groups of ADP appear to be scattered due to the flexibility of the rotatable bonds. The adenine ring nitrogen forms a hydrogen bond with the N–H of hinge residue L141, and the exocyclic amine makes a hydrogen bond with the backbone carbonyl oxygen atom of E139 in the hinge region. The phosphate groups are stabilized by strong interactions with I74, K93, N191 and D207. We have also done some other validation studies with Staurosporin, inhibitor **5**, **6** and **7**. Surflex reproduced the co-crystal conformations in their corresponding MK2 protein for all. We have docked other MK2 reported inhibitors in developed docking model to further enhance confidence in our docking model. Surflex reproduced the conformation of Staurosporin. There is no crystal structure information available for inhibitor **8**, but it is structurally similar to inhibitors **6** and **7**. So we assumed that it will orient in similar manner in the active site as inhibitors **6** and **7**. Putative conformation of inhibitor **8** in developed docking model is shown in Fig. 4a.

The docking study enhanced our confidence in applying the Surflex module for predicting the binding conformation and nature of interaction of other molecules such as the pyrazolo[1,5-*a*]-pyridine inhibitors [15] reported in patent (WO2006/109867A1). A set of structurally diverse but representative molecules as shown in Fig. 5 was selected with different ranges of activity, i.e. <0.2 μM (++++), 0.2–1 μM (+++), 1–10 μM (++), and 10–100 μM (+). These molecules were drawn in SYBYL7.3, Gasteiger–Huckel charges were added, and the molecules minimized using the Tripos force field until a conjugated gradient field reached up to 0.05 Å. The energy minimization guarantees a low-energy conformation with suitable bond distances and angles. The molecules were then docked in the same descriptor file (sfxc file) generated earlier. Various scores were calculated for each conformation of the inhibitors and conformations were sorted primarily on the basis of consensus of the individual score, and secondarily on the basis of the total score. In our study, we observed that sum of force field based scores, D-score (Dock score, component of DOCK docking program) and G-score (Gold score component of GOLD docking program) were able to discriminate between active vs inactive molecules as compared to other scoring functions such as Total_Score, PMF_Score and ChemScore.

D-score considers mainly the electrostatic and hydrophobic contributions to energy but not entropic terms. G-score emphasizes more on hydrogen-bonding interactions, which is expected to perform when significant polar interactions are present between the protein and ligand. PMF_Score more focused on the protein–ligand atom-pair interaction potentials derived from crystallographic data. ChemScore comes from a diverse training set of 82 protein–ligand complexes from the Protein Data Bank that whose value is derived from parameters of lipophilic, metal–ligand, hydrogen bonding, and rigid ligand nature. Total_Score is nothing but the FlexX_Score.

3.4. Analysis of docking results

We observed two binding conformations for molecule **9** having activities less than 0.2 μM (++++). In the 1st binding conformation (as shown in Fig. 6a), the nitrogen atom (1st position) of the pyrazole ring makes a hydrogen-bonding interaction with the hinge residue L141; the N-hydrogen at the 7th position of the pyrazolopyridine makes a second hydrogen bond with the backbone carbonyl oxygen of L141; the phenyl ring is stabilized by hydrophobic interactions with the side chain of L70; and the 4-ethoxyphenyl ring is oriented towards the solvent exposed region. The nitrogen atom of the nitrile appears to form a salt bridge interaction with the conserved K93. The 4-aminocyclohexyl group orients towards the phosphate-binding region and makes a strong ionic lock interaction with the conserved residue D207 (the first residue of the DFG motif) and a hydrogen-bonding interaction with the side chain of N191. In addition, molecule **9** also forms a close van der Waals interaction with several protein residues in the active site including the gatekeeper residue M138, and is stabilized by hydrophobic interactions with the side chains of the residues L70, V78, A91, and L193. About fifty percent of the conformations orient in the same way with a total score of 4.2 and a sum of force field based (D + G) scoring function of −149.0.

In the 2nd binding conformation of molecule **9** (as shown in Fig. 6b), the nitrogen atom of the nitrile forms a hydrogen-bonding interaction with the hinge residue L141. The *p*-ethoxyphenyl group orients towards the phosphate-binding region, with its oxygen atom forming a hydrogen bond with the N–H of K93. The phenyl ring also appears to be stabilized by the side chain of K93 through a cation–Π interaction. The 4-aminocyclohexyl ring orients towards the solvent exposed region, with its linker amine acting as a hydrogen bond donor to the backbone carbonyl oxygen atom of L141. Other residues of MK2 which are involved in van der Waals and hydrophobic stabilizing interactions with the inhibitor are L70, V78, A91, M138, and L193. In this 2nd binding conformation, the nitrile and the primary amino group on the cyclohexyl ring make no salt bridge interactions with the conserved K93 or D207. About forty-five percent of the conformations were oriented in this

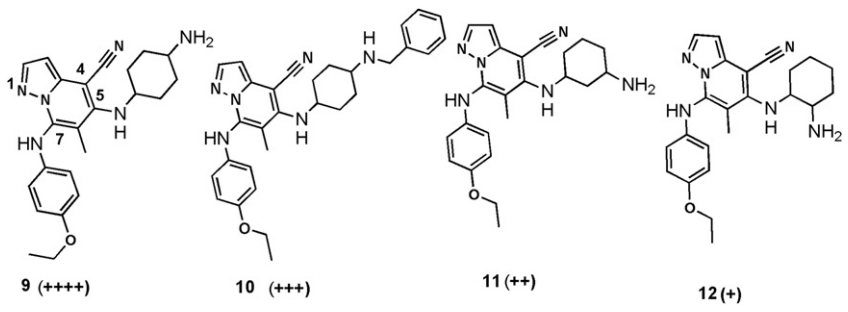

Fig. 5. Representative molecules used in the docking study, along with their activity codes in parentheses.

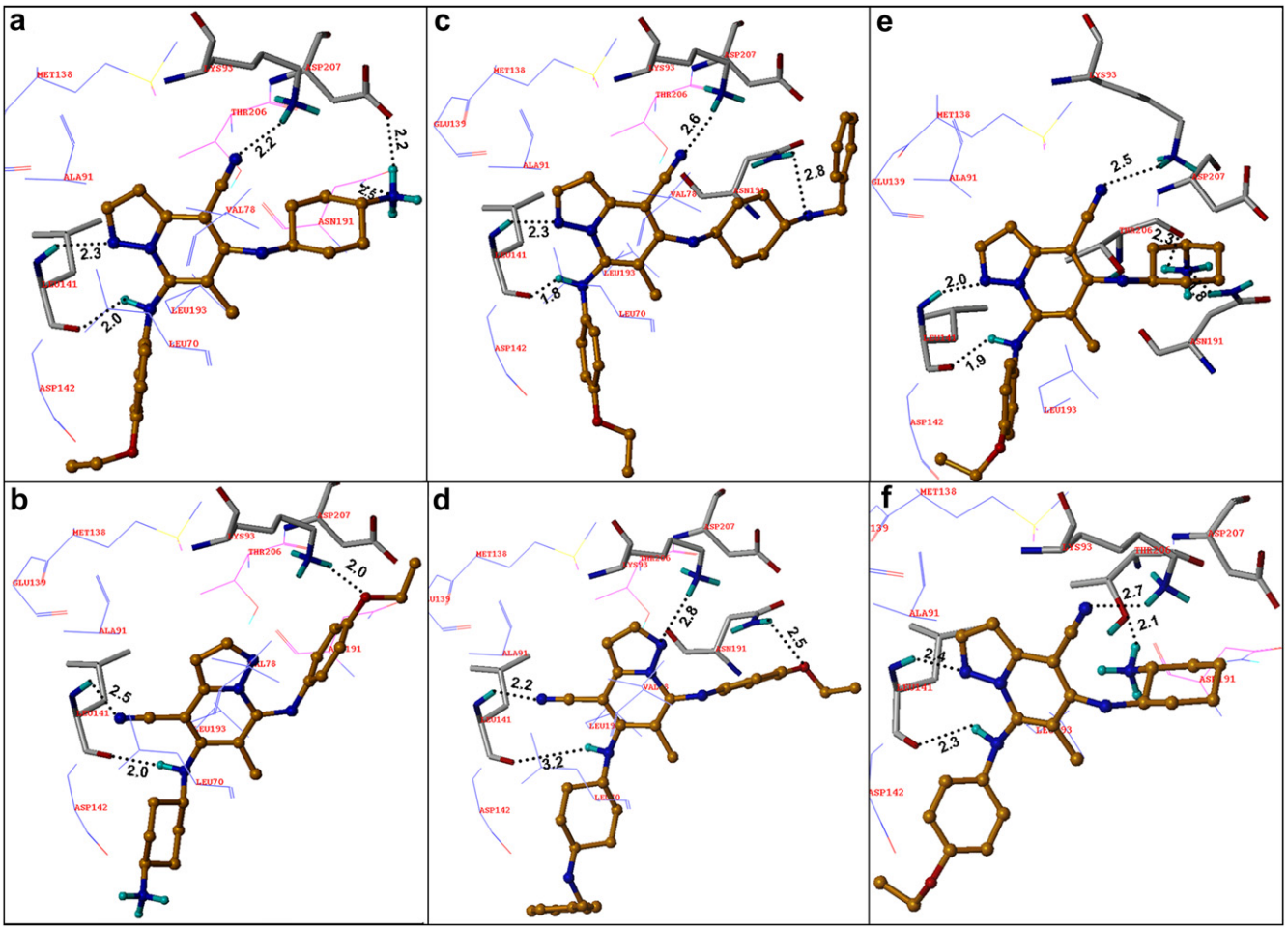

Fig. 6. (a) Putative binding conformation 1 of molecule **9**. (b) Putative binding conformation 2 of molecule **9**. (c) Putative binding conformation 1 of molecule **10**. (d) Putative binding conformation 2 of molecule **10**. (e) Putative binding conformation of molecule **11**. (f) Putative binding conformation of molecule **12**. Critical protein residues are colored in atom type stick model, other residues involved in van der Waal and hydrophobic interactions shown in blue, line model. Molecules shown in atom type, ball-and-stick model. Hydrogen-bonding interactions are shown in black dotted lines with corresponding distances.

manner with a total score of 4.6 and a sum of force field based (D + G) scores of −103.3.

A comparison of the 1st binding conformation of molecule **9** with the binding conformations of inhibitors **5**, **6**, **7** and **8** indicates the existence of common hydrogen-bonding interaction pattern with the residues K93, L141 and D207 of MK2. Solvent exposed substituents, i.e. the thiazole of inhibitor **5**, the quinoline of inhibitors **6** and **8**, and the phenyl group of inhibitors **7** and **9**, are stabilized by hydrophobic interactions with the side chain of L70 and the backbone carbonyl group of D142. Other ligand substituents which are stabilized by residues L70, V78, A91, L193, T206, and the gatekeeper M138 include the carboline ring of inhibitor **5**, the pyridine ring of inhibitors **6**, **7** and **8**, the pyrrole and pyrazole ring of inhibitors **7** and **8**, respectively, and the pyrazolopyridine ring of inhibitor **9**.

Molecule **10** selected from the second group (+++) shows two binding poses similar to those of molecule **9**. Molecule **10** in its 1st binding conformation (Fig. 6c) shows similar interactions to that of molecule **9**, but with the absence of a strong salt bridge interactions between the primary basic amine group of the inhibitor and the side chain of D207, and with the presence of an additional hydrophobic interaction of the phenyl group of **10** with the side chains of D186 and L188. This binding conformation was expected because the only structural difference between these two molecules is the substituent (benzyl) present in molecule **10**. About forty percent of the conformations orient in the same direction with a total score for the topmost conformation of 4.2 with the sum of force field based (D + G) scoring function being −167.0.

In the 2nd binding conformation of inhibitor **10** (as shown in Fig. 6d), the nitrile group shows a hydrogen-bonding interaction with the hinge residue L141. However, it appears that the ligand is further away from the hinge than the inhibitor **9**, because the pyrazole ring nitrogen forms a hydrogen-bonding interaction with the ϵ-amino group of K93, and the ethoxy oxygen atom makes a hydrogen-bonding interaction with the side chain of N191. Inhibitor **10** has stabilizing interactions with the other hydrophobic residues of MK2, viz. L70, V78, M138, and L193. Sixty percent of the conformations were oriented in the same manner with a total score of 3.4 and the sum of force field based (D + G) scoring function of −145.5.

Examination of the binding conformations of molecules **11** and **12** from the third and fourth groups (as shown in Fig. 6e and f, respectively) indicates similar binding orientations as compared to the first binding conformation of molecule **9**. Molecule **11** possesses two chiral centers and we did not have any information regarding its chirality. So, we have docked all the possible isomers and observed that molecule with R, R stereochemistry at both chiral centers was preferred. All the conformations of both molecules (**11** and **12**) occupy a similar volume. Both the molecules show interactions with MK2 similar to the first binding conformation of

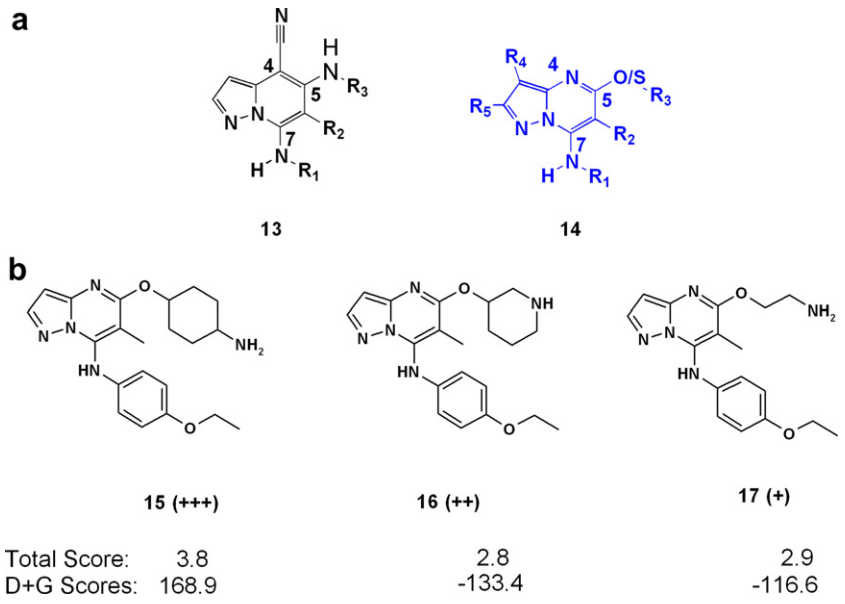

Fig. 7. (a) Structural differences in the pyrazolo[1,5-*a*]pyrimidine and the pyrazolo[1,5-*a*]pyridine cores. (b) Representative molecules used in the docking study, along activity codes in parentheses and total scores after consensus.

molecule **9**, but with the absence of the salt bridge with D207. The primary amino group of molecule **11** forms two hydrogen-bonding interactions with the side chains of N191 and T206, whilst the primary amino group of molecule **12** makes a hydrogen bond with the side chain of T206. The total scores of molecule **11** and **12** are 3.9 and 4.0, and the sum of force field based (D + G) scoring functions is −133.6 and −67.5, respectively.

The structure–activity relationships (SAR) and docking studies of molecules **9**–**12** indicate that the substitution at the 5th position of the pyrazolo[1,5-*a*]pyridine ring has a dramatic effect on activity. From docking, it is observed that in the first binding conformation of molecule **9**, a salt bridge interaction with the conserved D207 of MK2 occurs. Molecules **10**, **11**, **12** cannot form such an ionic interaction and are therefore less active than molecule **9**. As evident from docking, the substituent at the 7th position of the pyrazolopyridine ring orients towards the solvent exposed area, and the group next to linker nitrogen is involved in hydrophobic interactions. Moreover, the presence of different hydrophobic groups did not significantly affect MK2 inhibitory activity (Supplementary data sheet). Since the exact IC_{50} values for these molecules were not reported, we assume that the sum of the force field based scoring functions (D-score + G-score) offers an explanation of the differences in molecules activity except for molecule **10**. These functions can be explored further to segregate the molecules having different exact activity value.

The trend in the biological activities is difficult to explain with the second predicted binding conformation of molecules **9** and **10** (Fig. 6b and d). According to the second binding conformation of molecules **9** and **10**, the substituent at the 5th position orients towards the solvent exposed area and is not involved in direct interactions with any residues in the active site of MK2. By changing the group at this position, one should not expect a significant change in its inhibitory activity. On the contrary, this seems to be the only position that showed significant variation in activity (data shown in Supplementary data sheet). The *prima facie* evidence that this is not the case leads us to the inevitable

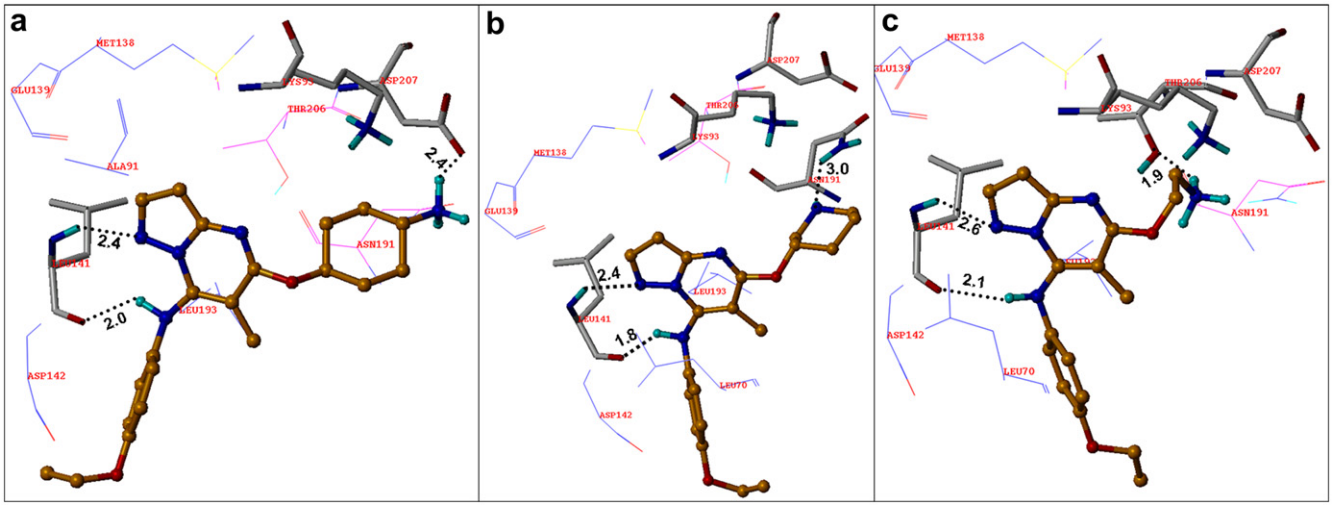

Fig. 8. Putative binding conformations of molecules **15** (a),**16** (b),**17** (c); orange; ball-and-stick model, critical protein residues are colored in atom type, stick model, other residues involved in van der Waal and hydrophobic interaction are shown in blue, line model. Hydrogen-bonding interactions are shown in black dotted lines with corresponding distances.

conclusion that the first binding conformation of molecules **9** and **10** is preferred over the second binding conformation, as corroborated by the sum of D and G scores.

To further strengthen our hypothesis, we analyzed another set of MK2 inhibitors from another patent, US2006/135514A1. [16] The overall structure of the compounds in both patents were similar, but the differences included: a pyrazolo[1,5-*a*]pyrimidine core in the second patent replacing the pyrazolo[1,5-*a*]pyridine in the first; a nitrogen atom replacing the nitrile group; and an oxygen or sulphur atom replacing the nitrogen atom in the linker at the 5th position, R4 and R5 are hydrogens in most of the pyrazolo[1,5-*a*]pyrimidine derivatives, except in some cases it is cyclopropyl (see compounds **13** and **14** in Fig. 7a). Although the structural differences between the molecules of both patents were small, the activity differences were large, with all the pyrazolo[1,5-*a*]pyrimidine ring containing molecules in the second patent being uniformly less potent than molecules containing the pyrazolopyridine ring. The structural similarity of the two series meant, however, that the binding conformations of the compounds from both patents should be similar within the MK2 active site.

To understand and explain the differences in the activities of the two series, we selected a few representative molecules (**15**, **16**, and **17**) from the second patent with activity ranges $\leq$2 μM (+++), 2–20 μM (++), and 20–100 μM (+), as shown in Fig. 7b. We did not have any information regarding chirality of molecule **16**. Hence, upon docking both the isomers we found that S stereoisomer is preferred over R stereoisomer.

The binding conformations of molecules **15**–**17** in MK2 were analyzed by adopting the same docking methodology as described earlier. The total score obtained for molecule **15** was 3.8 and the sum of the force field based (D + G) scoring function was −168.9, as shown in Fig. 7b. From the binding orientations of **15**, as shown in Fig. 8a, the nitrogen atom at the 1st position and the N–H at the 7th position of the pyrazolopyrimidine ring form the hinge interactions, and the *p*-ethoxyphenyl ring is exposed towards the solvent. The 4-aminocyclohexyl group orients towards the phosphate-binding region, with the primary amino group making a strong ionic lock interaction with the conserved residue D207 of the DFG motif: however, the amino group is 3.4 Å away from N191. In addition, this ligand forms close van der Waals interactions with several protein residues in the active site including the gatekeeper residue M138 and the hydrophobic side chains of L70, V78 and L193. This ligand shows a binding conformation and interactions similar to that of molecule **9** in its first binding conformation, apart from the absence of the nitrile–K93 interaction. The reason that molecule **15** is less active than molecule **9** may be attributed to the absence of the nitrile group which might otherwise make a salt bridge interaction with K93.

The orientation of molecules **16** and **17** (shown in Fig. 8b and c respectively) reveals binding conformations similar to molecule **9** with total scores of 2.8 and 2.9, and a sum of force field based (D + G) scoring functions of −133.4 and −116.6, respectively (Fig. 7b). Molecules **16** and **17** did not exhibit any ionic lock interactions with D207 because their primary amino groups were located remotely from the acidic side chain of aspartic acid.

In conclusion, the crystal structures of active and inactive forms of MK2 have been shown to have different active site shapes as implied from the different structural orientations of p-loop residues even though both forms have similar Ψ and Φ angles in their DFG motif. We propose plausible binding conformations of a number of different MK2 inhibitors, and suggest that the pyrazole nitrogen atoms of pyrazolo[1,5-*a*]pyridine and pyrazolo[1,5-*a*]pyrimidine classes of inhibitors make a hinge interaction with the MK2 enzyme.

Appendix. Supplementary data

Supplementary data associated with this article can be found in the online version, at doi:10.1016/j.ejmech.2009.09.030.

References

[1] L.J. Jeffrey, Curr. Top. Med. Chem. 7 (2007) 1313–1331.
[2] Z. Chen, T.B. Gibson, F. Robinson, L. Silvestro, G. Pearson, B. Xu, A. Wright, C. Vanderbilt, M.H. Cobb, Chem. Rev. 101 (2001) 2449–2476.
[3] J.C. Lee, J.T. Laydon, P.C. McDonnel, T.F. Gallagher, S. Kumar, D. Green, D. McNulty, M.J. Blumenthal, J.R. Heys, S.W. Landvatter, et al., Nature 372 (1994) 739–746.
[4] E. Haar, Structure 11 (2003) 611–612.
[5] P.P. Roux, J. Blenis, Microbiol. Mol. Biol. Rev. 68 (2004) 320–344.
[6] M. Gaestel, Nat. Rev. Mol. Cell Biol. 7 (2006) 120–130.
[7] F.G. Salituro, U.A. Germann, K.P. Wilson, G.W. Bemis, T. Fox, M.S. Su, Curr. Med. Chem. 6 (1999) 807–823.
[8] J. Kervinen, H. Ma, S. Bayoumy, C. Schubert, C. Milligan, F. Lewandowski, K. Moriarty, R.L. Desjarlais, K. Ramachandren, H. Wang, C.A. Harris, B. Grasberger, M. Todd, B.A. Springer, I. Deckman, Arch. Biochem. Biophys. 449 (2006) 47–56.
[9] A. Kotlyarov, Y. Yannoni, S. Fritz, K. Laass, J.B. Telliez, D. Pitman, L.L. Lin, M. Gaestel, Mol. Cell Biol. 22 (2002) 4827–4835.
[10] D. Stokoe, B. Caudwell, P.T. Cohen, P. Cohen, Biochem. J. 296 (1993) 843–849.
[11] D.R. Anderson, M.W. Mahoney, D.P. Phillion, T.E. Rogers, M.J. Meyers, G. Poda, S.G. Hegde, M. Singh, D.B. Reitz, K.K. Wu, I.P. Buchler, J. Xie, W.F. Vernier, WO 2004/058762 A1, 2004.
[12] P.G. Wyatt, A.L. Gill, G. Saxty, R. Apaya, WO/2005/014554, 2005.
[13] P.H. Olesen, A.R. Sorensen, WO/2004/099127, 2004.
[14] M.A. Dombroski, M.A. Letavic, K.F. Mcclure, WO/2004/020440, 2004.
[15] U. Gen, M. Yoshiyuki, M. Yohei, H. Motoko, K. Tomomi, T. Mika, M. Hiroaki, K. Kenichiro, Y. Yuko, WO2006/109867A1, 2006.
[16] K. Tomomi, I. Minoru, M. TakaKuwa, G. Unoki, et al., US 2006/135514A1, 2006.
[17] D.R. Anderson, S.G. Hegde, A.S. Kolodziej, E.J. Reinhard, W.F. Vernier, US 2005/6909001, 2005.
[18] D.R. Anderson, W.F. Vernier, L.F. Lee, E.J. Reinhard, S.G. Hegde, WO2004/054504A2, 2004.
[19] D.R. Anderson, S.G. Hegde, E.J. Reinhard, L. Gomez, W.F. Vernier, L.F. Lee, S. Liu, A. Sambandam, A.P. Snider, L. Masih, Bioorg. Med. Chem. Lett. 15 (2005) 1587–1590.
[20] D.R. Anderson, S. Nathan, A.S. Kolodziej, E.J. Reinhard, L.F. Lee, WO/2004/055015.
[21] C.E. Hanau, S.M. Mershon, M.J. Graneto, S.G. Hedge, M.J. Meyers, I.P. Buchler, K.K. Wun, S. Liu, K. Nacro, WO2004/058176 A2, 2004.
[22] D.R. Anderson, F.W. Vernier, W.M. Mahoney, G.R. Kurumbail, N. Caspers, I.G. Poda, F.J. Schindler, B.D. Reitz, J.R. Mourey, J. Med. Chem. 50 (2007) 2647–2654.
[23] J.P. Wu, J. Wang, A. Abeywardane, D.R. Andersen, M. Emmanuel, E. Gautschi, R.D. Goldberg, A.M. Kashem, S. Lukas, W. Mao, L. Martin, T. Morwick, N. Moss, C. Pargellis, R.U. Patel, L. Patnaude, W.G. Peet, D. Skow, R.J. Snow, Y. Ward, B. Werneburg, A. White, Bioorg. Med. Chem. Lett. 17 (2007) 4664–4669.
[24] A.N. Jain, J. Comput. Aided Mol. Des. 10 (1996) 427–440.
[25] A.N. Jain, J. Comput. Aided Mol. Des. 14 (2000) 199–213.
[26] J. Ruppert, W. Welch, A.N. Jain, Protein Sci. 6 (1997) 524–533.
[27] W. Welch, J. Ruppert, A.N. Jain, Chem. Biol. 3 (1996) 449–462.
[28] G. Jones, P. Willett, R.C. Glen, A.R. Leach, R.J. Taylor, Mol. Biol. 267 (1997) 727–748.
[29] H.M. Berman, J. Westbrook, Z. Feng, G. Gilliland, T.N. Bhat, H. Weissig, N.I. Shindyalov, E.P. Bourne, Nucleic Acids Res. 28 (2000) 235–242.
[30] R.G. Kurumbail, J.L. Pawlitz, R.A. Stegeman, W.C. Stallings, H.S. Shieh, R.J. Mourey, WO 2003/076333 A2, 2003.
[31] W. Meng, L.L. Swenson, M.J. Fitzgibbon, K. Hayakawa, E. Ter Haar, A.E. Behrens, R.J. Fulghum, A.J. Lippke, J. Biol. Chem. 277 (2002) 37401–37405.
[32] K.W. Underwood, K.D. Parris, E. Federico, L. Mosyak, R.M. Czerwinski, T. Shane, M. Taylor, K. Svenson, Y. Liu, C. Hsiao, S. Wolfrom, M. Maguire, K. Malakian, J. Telliez, L. Lin, W.R. Kriz, J. Seehra, S.W. Somers, L.M. Stahl, Structure 11 (2003) 627–636.
[33] C.R. Hillig, U. Eberspaecher, F. Monteclaro, M.J. Huber, D. Nguyen, A. Mengel, B. Muller-Tiemann, U. Egner, J. Mol. Biol. 369 (2007) 735–745.
[34] M. Huse, J. Kuriyan, Cell 109 (2002) 275–282.
[35] B. Nolen, S. Taylor, G. Ghosh, Mol. Cell 15 (2004) 661–675.
[36] R. Thaimattam, R. Banerjee, R. Miglani, J. Iqbal, Curr. Pharm. Des. 13 (2007) 2751–2765.